

MYOCARDIAL INFARCTION

Infarct Involution and Improved Function During Healing of Acute Myocardial Infarction: The Role of Microvascular Obstruction^{#,†}

**C. Joon Choi,¹ Shahriar Haji-Momenian,² Joseph M. DiMaria,²
Frederick H. Epstein,² Christina M. Bove,¹ Walter J. Rogers,^{1,2}
and Christopher M. Kramer, M.D.^{1,2,*}**

¹Department of Medicine, Cardiovascular Division and ²Department of Radiology,
University of Virginia Health System, Charlottesville, Virginia, USA

ABSTRACT

Delayed contrast-enhanced cardiac magnetic resonance imaging (ceCMR) delineates infarct size. The presence of hypoenhancement consistent with microvascular obstruction (MO) signifies larger infarcts with a worse prognosis. We hypothesized that the size of the contrast defect (CD) on ceCMR in acutely infarcted myocardium may change during infarct healing and depend upon the presence of MO. Twenty-five patients underwent CMR on weeks 1 and 8 after reperfused myocardial infarction. After short-axis cine CMR was performed, gadolinium was infused and ceCMR images and matched tagged cine MR images were obtained in the three most dysfunctional short-axis slices on cine CMR. The area and transmural extent of hyperenhancement (HE) with or without MO representing total CD size were planimetered. Between week 1 and week 8, the CD area fell from $1729 \pm 970 \text{ mm}^2$ at week 1 to $1270 \pm 706 \text{ mm}^2$ ($p < 0.001$), as did the transmural extent of infarction ($71 \pm 22\%$ to $63 \pm 24\%$, $p < 0.001$). The decline in CD trended to be higher in patients with MO ($840 \pm 807 \text{ mm}^2$) than in HE ($312 \pm 485 \text{ mm}^2$, $p < 0.07$). In the patient group as a whole, ejection fraction (EF) improved ($56 \pm 9\%$ to $60 \pm 10\%$, $p = 0.002$) between weeks 1 and 8, but patients with MO showed no increase in EF. Segments with some HE demonstrated partial functional improvement whereas no improvement was seen

[#]There is no conflict of interest or financial disclosure necessary on the part of any of the authors.

[†]Supported in part by grants from Berlex Laboratories, Inc. and the Entertainment Industry Foundation.

*Correspondence: Christopher M. Kramer, M.D., Department of Medicine and Radiology, University of Virginia Health System, Lee St., Box 800170, Charlottesville, VA 22908, USA; Fax: (434) 982-1618; E-mail: ckramer@virginia.edu.

in HE+MO segments. In patients 8 weeks after reperfused myocardial infarction (MI), the size of infarction by ceCMR decreases compared to week 1 post-MI, especially in those with microvascular obstruction in whom there is little improvement in regional or global function.

Key Words: Myocardial infarction; Magnetic resonance imaging; Myocardial contraction; Contrast media; Stunning; Myocardial.

INTRODUCTION

In patients with reperfused myocardial infarction, infarct size determines long-term prognosis (The Multi-center Postinfarction Research Group, 1983; Serruys et al., 1986). However, even in pathologic studies, exact estimates of infarct size change over time (Reimer and Jennings, 1979). Recently, contrast-enhanced cardiac magnetic resonance imaging (ceCMR) has been extensively validated in animal models (Kim et al., 1999) and humans (Wu et al., 2001) as a marker of the spatial location of the infarction and its transmural extent (Choi et al., 2001). Sequential studies in chronic infarction have demonstrated the reproducibility of delayed hyperenhancement between studies (Mahrholdt et al., 2002). However, serial studies with ceCMR after acute MI in patients have not been published to date.

Previous studies have demonstrated that infarcts with hypoenhancement at the core, generally surrounded by hyperenhanced myocardium, represent "microvascular obstruction" or MO (Judd et al., 1995) and are associated with larger infarcts (Lima et al., 1995). Infarcted regions with evidence of MO demonstrate less improvement of regional function (Kramer et al., 2000; Rogers et al., 1999) and worse long-term prognosis in terms of cardiac events (Wu et al., 1998a). We hypothesized that the size of the contrast defect (CD) on ceCMR in acutely infarcted myocardium may change during infarct healing and this change in size may depend upon the presence of MO.

METHODS

Study Patients

Twenty-five patients with a reperfused first myocardial infarction were prospectively enrolled in the study after informed consent was obtained. The protocol was approved by the Human Investigation Committee of the University of Virginia. Myocardial infarction (MI) was defined using typical chest pain longer than 30 minutes, electrocardiographic (ECG) changes of ST-segment deviation greater than 1 mm in

two or more contiguous leads, and troponin and/or CK-MB elevation $>2\times$ normal limit. Exclusion criteria included previous MI, unstable post-MI angina, NYHA class IV congestive heart failure, atrial fibrillation, aortic stenosis, sustained ventricular arrhythmia, inability to lay flat, or contraindication to cardiac magnetic resonance imaging (CMR) such as pacemakers, implantable defibrillators, or intracerebral aneurysm clips.

CMR

The patients were imaged lying supine in a Siemens Vision 1.5 T magnet using a phased-array surface coil overlying the anterior chest wall. After scout imaging, ECG-gated breath-hold gradient-echo cine imaging in the short-axis plane covering the left ventricle (LV) from apex to base was performed repetition time (TR) of 100 msec resulting in a 50 msec temporal resolution after view sharing; echo time (TE) of 4.8 msec; flip angle, 20 degrees; slice thickness, 7 mm; field of view (FOV) 30 cm; matrix, 126×256). Each breath-hold acquisition occurred over 15 heartbeats. Breath-hold tagged (Axel and Dougherty, 1989) cine imaging in three short-axis locations 10mm apart with the most dysfunctional regional wall motion seen on cine imaging was performed with 7-mm-thick short-axis slices using a segmented k-space tagged turbo-FLASH sequence with a temporal resolution of 45 msec (TR, 90 msec with view sharing; TE, 4 msec; 7 line segmentation; 8-mm tag line separations; 128×256 matrix interpolated to 256×256 ; FOV, 30 cm).

Contrast-enhanced cardiac magnetic resonance imaging was performed after infusion of 0.1 mM/kg Gd-DTPA (gadolinium-diethylenetriaminepentaacetic acid, gadopentate dimeglumine, Magnevist, Berlex, Wayne, NJ). Imaging was performed in the same three short axis images as imaged with tagging as above. Inversion-recovery turbo FLASH ceCMR (Simonetti et al., 2001) was performed in each of the 3 slices every 2 min up to 20 min postcontrast (TR, 1400 msec; TE, 3.4 msec; flip angle, 25 degrees; inversion time (TI) 200–250 msec; delay time, 300 msec; slice thickness, 5 mm; FOV, 30 cm; matrix, 165×256 ; every other beat for one breath hold). The TI was kept constant during the 20-min period.

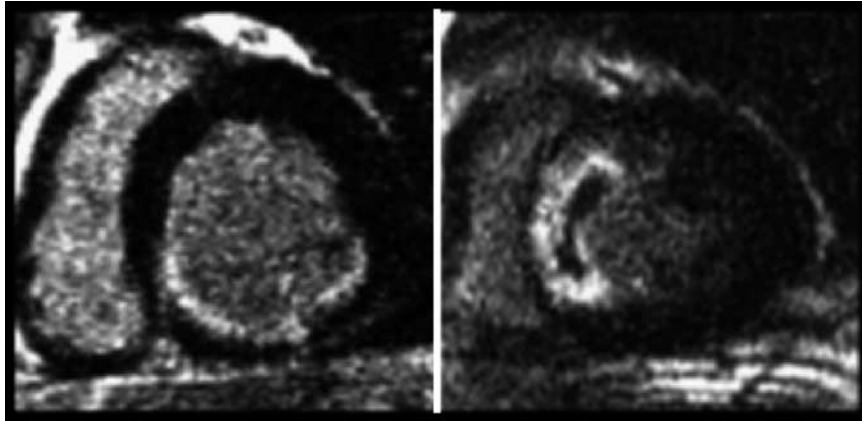


Figure 1. **Left panel.** Hyperenhanced subendocardium demonstrated in the inferior and posterior segments in a basal ventricular short-axis view after Gd-DTPA from a patient with a non-ST elevation myocardial infarction at week 1 post-MI. **Right panel.** Hypoenhanced core surrounded by hyperenhancement in a septal mid-ventricular segment obtained in another patient with reperfused anterior myocardial infarction at week 1 post-MI.

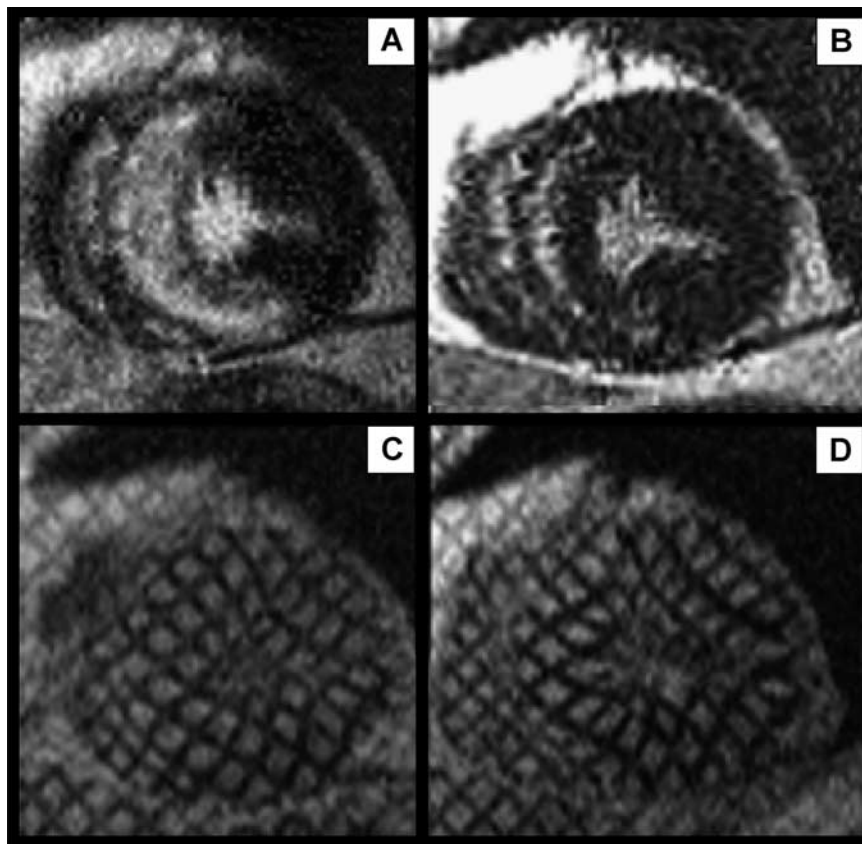


Figure 2. Four-panel figure from an MRI in a patient after anterior myocardial infarction reperfused with primary angioplasty. (A) Apical short-axis segmented inversion recovery image on day 4 post-MI after infusion of 0.1 mM/kg of Gd-DTPA. Note the large area of hyperenhancement in the septum. (B) The same apical short-axis image location at 8 weeks post-MI. Much of the hyperenhancement is no longer seen in the septum, leaving a nontransmural region of hyperenhancement, primarily in the subepicardium. (C) Apical short-axis end-systolic tagged gradient echo image at the same location at day 4 post-MI demonstrating markedly reduced tag deformation in the septum. (D) Apical short-axis end-systolic tagged gradient-echo image in the same location at 8 weeks post-MI, demonstrating recovery of tag stripe deformation throughout the septum, denoting recovery of regional function in that segment.

Follow-Up CMR

Eight weeks following MI, patients were brought back for a follow-up CMR study using the identical imaging protocol. The three short-axis slices imaged with ceCMR were matched to the week 1 post-MI image set using apex to base location, papillary muscles, and right ventricular insertion sites.

Image Analysis

Since the TI was kept constant during the postcontrast imaging, the time point with optimal nulling of noninfarcted myocardium between minute 2 and minute 20 postcontrast was selected by two investigators blinded to clinical information by consensus and only these images were analyzed for the size of the contrast defect. Serial postcontrast ceCMR images were aligned in one computer screen and the

same level of brightness and contrast applied to all images prior to analysis. The time point at which nulling of remote myocardium was optimal was on average 10.2 ± 2.2 minutes after contrast injection. Regions of hypoenhancement as a marker of microvascular obstruction (MO) (Judd et al., 1995; Wu et al., 1998a) were defined visually on these images (Fig. 1B). Regions with signal intensity, (Image J, NIH on a PC), of $>200\%$ of remote at this time point were defined as hyperenhanced (HE) from images obtained at both 1 and 8 weeks post-MI (Figs. 1A and 2). The area and transmural extent of HE with or without persistent MO representing total contrast defect (CD) size were planimeted. Transmural extent of the contrast defect across the myocardial wall was defined as in previous studies (Kim et al., 2000).

Percent circumferential intramyocardial shortening (%S) was measured in standard fashion (Kramer et al., 2000; Rogers et al., 1999) from tagged images by an

Table 1. Patient demographics.

Patient #	Age	Sex	Location	ST elevation	Peak TP-I	Reperfusion	Days to MRI	Beta-bl	ACE-I	Statin
1	55	M	Inferior	Y	49.3	1° PCI	2	Y	N	Y
2	50	M	Lateral	N	50	SR+2° PCI	4	N	N	Y
3	64	F	Inferior	Y	2.3	1° PCI	2	Y	Y	Y
4	44	M	Inferior	Y	43.5	1° PCI	3	Y	Y	Y
5	37	M	Inferior	N	52	SR+2° PCI	4	Y	Y	Y
6	62	M	Anterior	Y	CK (1010)	SR+2° PCI	7	N	Y	Y
7	62	M	Inferior	Y	54	1° PCI	3	Y	Y	Y
8	62	F	Inferior	Y	35.9	1° PCI	4	Y	Y	N
9	51	M	Anterior	Y	CK (1135)	Lytics+2° PCI	4	Y	Y	Y
10	51	M	Anterior	Y	117	Lytics+2° PCI	7	Y	Y	Y
11	56	M	Anterior	Y	6	Lytics+2° PCI	5	Y	Y	N
12	66	M	Inferior	Y	3	Lytics+2° PCI	4	N	Y	Y
13	52	M	Anterior	Y	49	1° PCI	5	Y	Y	Y
14	51	M	Anterior	Y	20	1° PCI	7	Y	Y	Y
15	50	M	Inferior	N	44	SR+2° PCI	3	Y	Y	N
16	53	M	Inferior	Y	140	1° PCI	3	Y	Y	N
17	68	M	Inferior	Y	92	1° PCI	5	N	Y	Y
18	52	M	Lateral	N	11	SR+2° PCI	6	Y	Y	Y
19	68	M	Anterior	Y	210.4	Lytics+2° PCI	3	Y	Y	Y
20	47	M	Anterior	Y	410.5	1° PCI	3	Y	Y	Y
21	46	M	Inferior	Y	202	Lytics+2° PCI	5	Y	Y	Y
22	53	M	Inferior	Y	331.6	Lytics+2° PCI	6	Y	N	Y
23	56	M	Anterior	Y	140.2	Lytics+2° PCI	5	Y	Y	Y
24	46	M	Inferior	Y	27	1° PCI	4	Y	Y	Y
25	46	M	Inferior	N	17	SR+2° PCI	3	Y	Y	Y
All (mean±SD)	53±8	NA	NA	NA	93±106	NA	4±2	NA	NA	NA

Abbreviations: M=male; F=female; Y=yes; N=no; TP-I=troponin-I (ng/ml); CK=creatinine kinase (IU/L); 1° (primary) and 2° (rescue) PCI=primary and rescue percutaneous coronary intervention; SR=spontaneous reperfusion; Lytics=thrombolytics; Beta-bl=beta-blocker; ACE-I=angiotensin converting enzyme inhibitor.

investigator blinded to results of the contrast images using the VIDA software package (© Univ. of Iowa) on a Sun UltraSparc 10 workstation within the subendocardium and subepicardium in 4 sectors (anteroseptal, anterolateral, inferolateral, and inferoseptal), for a total of 8 segments per slice. The same analysis was repeated on corresponding slices on the 8-week post-MI study.

Global LV volumes and mass at both time points were measured from end-diastolic and end-systolic volumes from stacked short-axis cine images planimetered by an investigator blinded to the contrast-enhanced data using Argus software (Siemens, Princeton, NJ).

Statistical Analysis

The temporal changes in CD area, transmural extent, global LV volumes, mass, and function between weeks 1 and 8 post-MI, %S in the subendocardium and subepicardium were compared by Student's Paired T-Test for the entire patient group. Differences in these parameters at a single point in time were compared between type of contrast pattern (HE vs. HE + MO) by an unpaired T-Test. Two-way analysis of variance (ANOVA) was used to compare changes in regional function by location and time point.

RESULTS

Patient Population

Twenty-five patients, 23 males and 2 females, mean±SD age, 53±8 years, were studied by CMR on day 4±2 (Wk 1) and week 8±1 (Wk 8) after reperfused first MI (Table 1). All patients had a patent

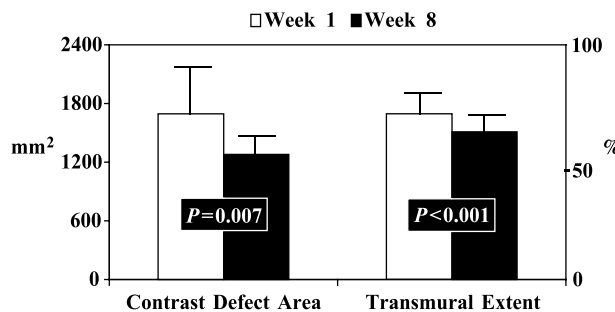


Figure 3. Graph depicting the change in the area (left y-axis) and transmural extent of the contrast defect (right y-axis) between week 1 and 8 post-MI from the 3 short-axis slices. White bars represent data at 1 week and black bars data at 8 weeks post-MI.

Table 2. Changes in LV size and global function between week 1 and 8 post-MI by type of contrast defect.

		Week 1	Week 8
LVEDV (ml)	HE	91±24	98±27†
	HE+MO	115±46	134±67
LVESV (ml)	HE	37±25	35±27
	HE+MO	52±41*	55±42*
LVEF (%)	HE	58±7	63±7†
	HE+MO	49±10*	51±10*
LV mass (g)	HE	171±49	167±59
	HE+MO	194±67	190±35

*p<0.05 vs. HE.

†p<0.05 vs. week 1.

infarct-related coronary artery as defined by coronary angiography at the time of Wk 1 CMR study after reperfusion achieved either by thrombolysis or percutaneous coronary intervention. Nine patients suffered anterior and 11 inferior ST elevation MI and another 5 had non-ST elevation MI, all of which were inferior or lateral. Twelve patients received primary stenting, seven patients thrombolysis (4 of them followed by rescue stenting), and six reperfused spontaneously and received delayed stenting. Average peak troponin-I was 93±106 µg/L.

Area of Contrast Defect

The total CD area fell from 1729±980 mm² at Wk 1 to 1270±706 mm² at Wk 8 (p<0.001), as did the transmural extent (71±22% to 63±24%, respectively, p<0.001) (Fig. 3). Eighteen patients showed HE only and seven patients HE+MO at Wk 1. All areas of MO were surrounded by regions of HE. The CD area in HE fell from 1496±767 mm² at Wk 1 to 1184±714 mm² at Wk 8 (p<0.03) and in HE+MO from 2329±1230 mm² at Wk 1 to 1489±685 mm² at Wk 8, p<0.04). The decline in CD area tended to be greater in patients with HE+MO (840±807 mm²) than in patients with MO (312±485, p<0.07). The transmural extent decreased over time both in HE and in HE+MO (66±20% at Wk 1 to 62±22% at Wk 8 in HE, 81±22% at Wk 1 to 65±28% at Wk 8 in HE+MO, p<0.005 for each). The decline in transmural extent was greater in HE+MO (16±15%) than for HE (4±9%, p<0.001).

Global LV Size and Function

In all 25 patients, neither LV mass (177±55 g to 173±55 g) nor end-systolic volume (44±21 ml to

45±32 ml) changed between weeks 1 and 8, but end-diastolic volume increased (97±33 ml to 108±45 ml, $p=0.02$) and EF improved (56±9% to 60±10%, $p=0.002$). The lack of change in total LV mass implies some increase in the mass of noninfarcted myocardium, since there was a loss of mass of infarcted myocardium as demonstrated by the reduction in CD size.

The data comparing global LV size and function between patients with HE and HE+MO is shown in Table 2. Patients with HE+MO had worse LV function both at week 1 and week 8 as evidenced by higher LVESV and lower LVEF at both time points. Ejection fraction improved between week 1 and 8 only in the group with HE, in which LVEDV increased but LVESV remained unchanged (Table 2).

Regional LV Function

From the contrast-enhanced MR images and matched tagged images at week 1, a total of 132 tagged segments were located within a contrast defect and 102 segments were remote. Of the 132 tagged segments, 91 were subendocardial and 41 subepicardial. The 18 patients with HE demonstrated 73 tagged segments within regions of hyperenhancement, 60 of which were subendocardial and 13 subepicardial. The seven patients with HE+MO had 59 tagged segments within the contrast defect, 31 subendocardial, and 28 subepicardial at week 1 post-MI.

Regional %S from all 132 infarcted segments improved from 6.9±7.4% at Wk 1 to 12.1±10.5% at Wk 8, $p<0.001$. Changes in regional %S between week

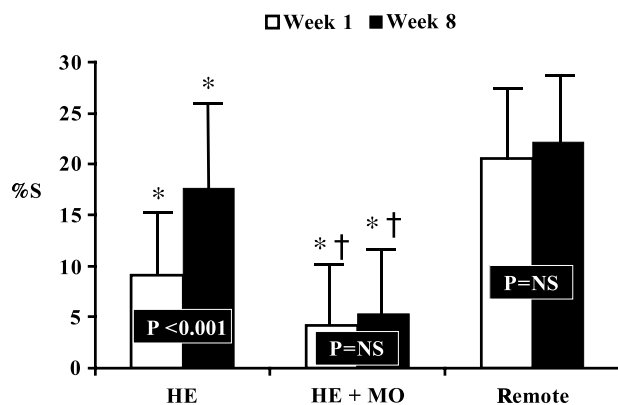


Figure 4. Changes in circumferential shortening (%S) in hyperenhanced regions (HE), regions with hyperenhancement and microvascular obstruction (HE+MO), and remote regions between week 1 and 8 post-MI. White bars represent data at 1 week and black bars data at 8 weeks post-MI. * $p<0.05$ vs. remote; † $p<0.05$ vs. HE.

Table 3. Circumferential shortening of subendocardium and subepicardium at week 1 and 8 postinfarction in hyperenhanced (HE), hyperenhanced with hypoenhanced (HE+HO), and remote (RM) regions.

Location	Week 1 (%)	Week 8 (%)	<i>p</i> value
Subendocardium			
HE, n=60	10.2±7.1*	19.0±9.3*	<0.001
HE+MO, n=31	5.9±5.8*†	7.3±6.9*†	NS
remote, n=52	24.1±5.7	26.9±6.1	0.014
Subepicardium			
HE, n=13	4.0±8.7*	11.5±8.9	0.04
HE+MO, n=28	2.3±6.0*	3.0±6.6*†	NS
remote, n=50	16.8±6.2	17.3±5.7	NS

* $p<0.05$ vs. remote.

† $p<0.05$ vs. HE.

1 and week 8 by contrast pattern are shown in Fig. 4. Percent S in both HE and HE+MO (9.1±2.7% and 4.2±6.1%, respectively) was depressed at Wk 1 post-MI compared to remote (20.5±6.9%, ANOVA $p<0.001$). By week 8, %S improved in HE regions (9.1±2.7% at Wk 1 to 17.6±9.6% at Wk 8, $p<0.001$), but did not improve in HE+MO (4.2±6.1% at Wk 1 to 5.3±7.1% at Wk 8, $p=NS$). At week 8, %S in HE was better than HE+MO, but remained less than remote (17.6±9.6%, 5.3±7.1%, 22.2±7.6% respectively, ANOVA $p<0.001$) (Fig. 4).

Differential improvement based on contrast defect pattern was consistent by transmural location (Table 3). Within the subendocardium at week 1, there was a gradient in %S between HE segments (10.2±7.1%), HE+MO segments (5.9±5.8%), and remote (24.1±5.7%, $p<0.001$). By 8 weeks post-MI, subendocardial function in HE segments had improved (10.2±19.0% at Wk 1 to 26.9±6.1% at Wk 8, $p<0.001$), but remained depressed in HE+MO segments (5.9±5.8% at Wk 1 to 7.3±6.9% at Wk 8, $p=NS$). In subepicardial segments at week 1, %S was depressed in both HE and HE+MO compared to remote (4.0±8.7%, 2.3±6.0%, 16.8±6.2%, respectively, $p<0.001$). By eight weeks post-MI, subepicardial function in HE had improved (4.0±8.7% at Wk 1 to 11.5±8.9% at Wk 8, $p=0.04$), but remained depressed in HE+MO (2.3±6.0% at Wk 1 to 3.0±6.6% at Wk 8, $p=NS$).

DISCUSSION

This study demonstrates that the size of myocardial infarction as assessed by ceCMR decreases over

eight weeks post-MI in patients with first reperfused myocardial infarction. A 26% decrease in the size of the contrast defect area and an 11% decrease in its transmural extent during infarct healing were found. Patients with evidence of microvascular obstruction in the first week after reperfusion had larger infarct size with greater transmural involvement as well as lower ejection fraction than those with HE alone. In addition, these patients demonstrated less regional functional improvement within the infarct zone and less improvement in global LV function. During infarct healing, infarcts with MO showed a greater decline in infarct transmural extent and showed a trend toward a greater decline in the mass of infarcted tissue. This higher extent of infarct involution in infarcts with MO is likely related to greater initial damage, especially to the microvasculature.

A decline in the size of infarction after the first few days has been demonstrated in prior canine pathologic studies (Reimer and Jennings, 1979). These investigators demonstrated that the average infarct size at 4 days after circumflex occlusion was 41% of the LV, whereas by day 28, only 11% of the LV was infarcted and replaced by dense scar. The larger infarct size measured at 4 days post-MI was due to a 25% increase in infarct water content as well as hemorrhage and inflammation (Reimer and Jennings, 1979). The investigators concluded that early infarct volume is overestimated relative to tissue weight and underestimated at the week 4 time point. Much of the decline in the area of the contrast defect from day 4 to week 8 seen in the present study may be due to infarct involution with a relatively small contribution from resolution of the edema and hemorrhage that characterizes the periphery of acute infarction.

In a canine model using the segmented inversion recovery sequence recently described and used in this study, Kim et al. (1999) confirmed an excellent match between infarct area by triphenyltetrazolium chloride (TTC)-stained slices and ceCMR when MR images were acquired 30 min after infusion of high dose (0.3 mM/kg) Gd-DTPA. An earlier study from the same group using contrast-enhanced CMR, but an older imaging sequence, showed a 12% overestimation of MI size defined by TTC staining (Judd et al., 1995). Possible explanations include the sequence used, partial volume effects, peri-infarct edema and inflammation, or intrinsic limitations of the TTC staining method (Wu et al., 1999).

The present study agrees with a previous canine study that showed a reduction in the area of hyperenhancement during infarct healing (Kim et al., 1999). In five animals imaged at both 3 days and 8 weeks

post-MI in that study, the absolute volume of the hyperenhanced region on ceCMR decreased by a factor of 3.4 ± 1.4 from day 3 to week 8 while the volume of nonhyperenhanced regions increased by 1.2 ± 0.2 . This suggests involution of the infarct area during infarct healing as well as hypertrophy of noninfarcted myocardium that characterizes postinfarct LV remodeling (Kramer et al., 1993). In the present study, LV mass didn't change, despite the fall in mass of infarcted tissue, suggesting some hypertrophy of noninfarcted myocardium.

Evidence of microvascular obstruction on the week 1 study is a marker for larger infarction with a worse prognosis, as shown previously (Lima et al., 1995; Wu et al., 1998a). Compared to these previous studies that used first-pass or delayed enhancement images in the first 3 min after contrast to define MO, our study imaged MO at approximately 10 min postgadolinium. The areas of MO in the present study likely represent the most dense regions of MO, those that do not fill in with contrast by 10 min. Previous canine studies have shown that the size of hypoenhancement increases significantly over the first 48 hr after MI (Rochitte et al., 1998), but remains unchanged between days 2 and 9 post-MI (Wu et al., 1998b). The present study adds to the understanding of the natural history of infarcts with MO, demonstrating that there is significant loss of myocardial mass within those segments during infarct healing, likely due to involution/cellular loss.

The findings relative to changes in regional function extend those made in earlier studies from our group (Kramer et al., 2000; Rogers et al., 1999). For one, a newer inversion recovery sequence (Simonetti et al., 2001) was used to maximize visualization and quantitation of infarct size. With the addition of contrast-enhanced imaging at 8 weeks post-MI, temporal changes in infarct size were seen. Regional functional improvement was related to the presence or absence of microvascular obstruction, consistent with prior studies. Our findings agree with those of Gerber et al. (2002). In addition to demonstrating that dysfunctional regions without delayed hyperenhancement were the most accurate at predicting functional improvement, these investigators showed some improvement in function within regions of delayed hyperenhancement over time.

Limitations

Only three slices with the most dysfunctional wall motion on cine CMR were imaged by ceCMR during each scan. Therefore, total infarct size (% of LV mass) was not measured. These slices are representative of the center of the infarct due to the significant regional

dysfunction. Since the entire LV was not covered by ceCMR, the possibility of mismatch of short-axis locations from Wk 1 to Wk 8 exists. However, locations were carefully matched between time points using apex-to-base location, papillary muscles, and RV insertion points as done in prior studies (Kramer et al., 2000; Rogers et al., 1999). In addition, LV mass did not change over the course of the study, suggesting little global LV remodeling, and facilitating the matching process. These data may not be extrapolated to patients with severe LV dysfunction post-MI or prior to MI. Improvement of contractile function may be incomplete at the follow-up time point chosen for this study (8 weeks post-MI). The smaller size of the group with MO may limit the power to detect changes between groups.

The degree of infarct involution in the presence of MO tended to be greater than that in the absence of MO but this difference failed to reach statistical significance. Therefore, it cannot be excluded that a larger infarct size in and of itself may lead to greater involution even without the presence of MO.

CONCLUSIONS

The size and transmural extent of reperfused infarction in humans decreases from the first week to week 8 post-MI as characterized by contrast-enhanced CMR. This is especially true in infarcts with evidence of microvascular obstruction. Regional and global function improves to some extent in those infarcts without MO. Potential mechanisms for the decrement in infarct size in reperfused infarction include primarily infarct involution but may also in part reflect resolution of tissue edema and hemorrhage in the periphery of the acute infarct.

ACKNOWLEDGMENTS

The authors thank Jennifer R. Hunter, R.N., for patient scheduling and John M. Christopher, R.T., for performance of the MR imaging.

REFERENCES

- Axel, L., Dougherty, L. (1989). Magnetic resonance imaging of motion with spatial modulation of magnetization. *Radiology* 171:841–845.
- Choi, K. M., Kim, R. J., Gubernikoff, G., Vargas, J. D., Parker, M., Judd, R. M. (2001). Transmural extent of acute myocardial infarction predicts long-term improvement in contractile function. *Circulation* 104:1101–1107.
- Gerber, B. L., Garot, J., Bluemke, D. A., Wu, K. C., Lima, J. A. (2002). Accuracy of contrast-enhanced magnetic resonance imaging in predicting improvement of regional myocardial function in patients after acute myocardial infarction. *Circulation* 106:1083–1089.
- Judd, R. M., Lugo-Olivieri, C., Arai, M., Kondo, T., Croisille, P., Lima, J. A., Mohan, V., Becker, L. C., Zerhouni, E. A. (1995). Physiological basis of myocardial contrast enhancement in fast magnetic resonance images of 2-day-old reperfused canine infarcts. *Circulation* 92:1902–1910.
- Kim, R. J., Fieno, D. S., Parrish, T. B., Harris, K., Chen, E.-L., Simonetti, O., Bundy, J., Finn, J. P., Klocke, F. J., Judd, R. M. (1999). Relationship of MRI delayed contrast enhancement to irreversible injury, infarct age and contractile function. *Circulation* 100:1992–2002.
- Kim, R. J., Wu, E., Rafael, A., Chen, E.-L., Parker, M., Judd, R. M. (2000). The use of contrast-enhanced magnetic resonance imaging to identify reversible myocardial dysfunction. *N. Engl. J. Med.* 343:1445–1453.
- Kramer, C. M., Lima, J. A., Reichek, N., Ferrari, V. A., Llaneras, M. R., Palmon, L. C., Yeh, I.-T., Tallant, B., Axel, L. (1993). Regional function within noninfarcted myocardium during left ventricular remodeling. *Circulation* 93:1279–1288.
- Kramer, C. M., Rogers, W. J. Jr., Mankad, S., Theobald, T., Pakstis, D., Hu, Y.-L. (2000). Contractile reserve and contrast uptake patterns by magnetic resonance imaging and functional recovery after reperfused myocardial infarction. *J. Am. Coll. Cardiol.* 36:1835–1840.
- Lima, J. A., Judd, R. M., Bazille, A., Schulman, S. P., Atalar, E., Zerhouni, E. A. (1995). Regional heterogeneity of human myocardial infarcts demonstrated by contrast-enhanced MRI: potential mechanisms. *Circulation* 92:1117–1125.
- Mahrholdt, H., Wagner, A., Holly, T. A., Elliott, M. D., Bonow, R. O., Kim, R. J., Judd, R. M. (2002). Reproducibility of chronic infarct size measurement by contrast-enhanced magnetic resonance imaging. *Circulation* 106:2322–2327.
- Reimer, K. A., Jennings, R. B. (1979). The changing anatomic reference base of evolving myocardial infarction. *Circulation* 60:866–876.
- Rochitte, C. E., Lima, J. A., Bluemke, D. A., Reeder, S. B., McVeigh, E. R., Furuta, T., Becker, L. C.,

- Melin, J. A. (1998). Magnitude and time course of microvascular obstruction and tissue injury after acute myocardial infarction. *Circulation* 98:1006–1014.
- Rogers, W. J. Jr., Kramer, C. M., Geskin, G., Hu, Y.-L., Theobald, T.-M., Vido, D. A., Petruolo, S., Reichel, N. (1999). Early contrast-enhanced MRI predicts late functional recovery after reperfused myocardial infarction. *Circulation* 99:744–750.
- Serruys, P. W., Simoons, M. L., Suryapranata, H., Vermeer, F., Wijns, W., van den Brand, M., Bar, F., Zwaan, C., Krauss, X. H., Remme, W. J. (1986). Preservation of global and regional left ventricular function after early thrombolysis in acute myocardial infarction. *J. Am. Coll. Cardiol.* 7:729–742.
- Simonetti, O. P., Kim, R. J., Fieno, D. S., Hillenbrand, H. B., Wu, E., Bundy, J. M., Finn, J. P., Judd, R. M. (2001). An improved MR imaging technique for the visualization of myocardial infarction. *Radiology* 218:215–223.
- The Multicenter Postinfarction Research Group. (1983). Risk stratification and survival after myocardial infarction. *N. Engl. J. Med.* 309:331–336.
- Wu, K. C., Zerhouni, E. A., Judd, R. M., Lugo-Olivieri, C. H., Barouch, L. A., Schulman, S. P., Blumenthal, R. S., Lima, J. A. (1998a). Prognostic significance of microvascular obstruction by magnetic resonance imaging in patients with acute myocardial infarction. *Circulation* 97:765–772.
- Wu, K. C., Kim, R. J., Bluemke, D. A., Rochitte, C. E., Zerhouni, E. A., Becker, L. C., Lima, J. A. (1998b). Quantification and time course of microvascular obstruction by contrast-enhanced echocardiography and magnetic resonance imaging following acute myocardial infarction and reperfusion. *J. Am. Coll. Cardiol.* 32:1756–1764.
- Wu, K. C., Rochitte, C. E., Lima, J. A. (1999). Magnetic resonance imaging in acute myocardial infarction. *Curr. Opin. Cardiol.* 14:480–484.
- Wu, E., Judd, R. M., Vargas, J. D., Klocke, F. J., Bonow, R. O., Kim, R. J. (2001). Visualisation of presence, location, and transmural extent of healed Q-wave and non-Q-wave myocardial infarction. *Lancet* 357:21–28.

Submitted December 4, 2003

Accepted May 5, 2004